

# GLOBULES, DARK CLOUDS, AND LOW MASS PRE-MAIN SEQUENCE STARS

A. R. Hyland  
Mount Stromlo and Siding Spring Observatories  
The Australian National University  
Canberra, Australia

## ABSTRACT

The current observational and theoretical literature on Bok globules and their relationship to star formation is reviewed. Recent observations of globules at optical, infrared, and far infrared wavelengths are shown to provide important constraints on their structure and evolutionary status, and the suggestion that many globules are gravitationally unstable is seriously questioned.

Dark clouds associated with T associations are well-known sites of recent and continuing star formation. In recent years molecular observations and far infrared surveys have provided maps of such regions from which possible sites of star formation may be identified. Optical ( $H\alpha$ ) and near infrared surveys have enabled a clear identification of pre-main sequence (PMS) objects within the clouds. Methods of distinguishing these from background objects and the nature of their infrared excesses are examined in the light of recent observations in the near and far infrared. The perennial question as to the existence of anomalous reddening within dark clouds is also investigated.

## 1. GLOBULES

The large globules (Bok and Reilly 1947) are fascinating to observer and theoretician alike, for, although their status is not crystal clear, recent evidence from optical and radio studies (e.g., Dickman 1977) suggests that the majority of globules are in a state of gravitational collapse, which may eventually lead to star formation (Bok 1977).

There is also direct observational evidence on this question to be drawn from the discovery by Herbst and Turner (1976) of possible embedded sources in Lynds 810, and the association of two Herbig-Haro objects with the southern globule 210-6A (Schwartz 1977; Bok 1978). On the theoretical side, there are certain difficulties in collapse

calculations, which have been succinctly spelled out by Buff *et al.* (1979), who conclude that "[given the practical impossibility of knowing the initial spectrum of perturbations] there will be no unique solution for a collapsing cloud."

With these problems in mind it would appear that increased knowledge of the evolutionary status of globules depends to a large extent on continuing observational studies. It is important, therefore, that these observational studies be able to determine the correct physical parameters for the globules, which is not as simple as might be supposed.

### 1.1 Description and Methods of Study

The large globules are generally round in appearance, dense (i.e., opaque), and come in a variety of apparent sizes from a few minutes to half a degree in diameter. Photographs of a selection of globules are given by Bok (1977) and Bok *et al.* (1971), and in Figure 1, Coalsack globules 1, 2, and 3 (Bok *et al.* 1977) are shown.

Typical methods of study in the optical are from the reddening of background objects, and a variety of methods of star counts. These have been beautifully summarised by Bok and Cordwell (1973), and have been the basis for most optically determined parameters for globules, e.g., Bok and McCarthy 1974; Tomita *et al.* 1979; Schmidt 1975. Unfortunately, the single direct method of determining the density

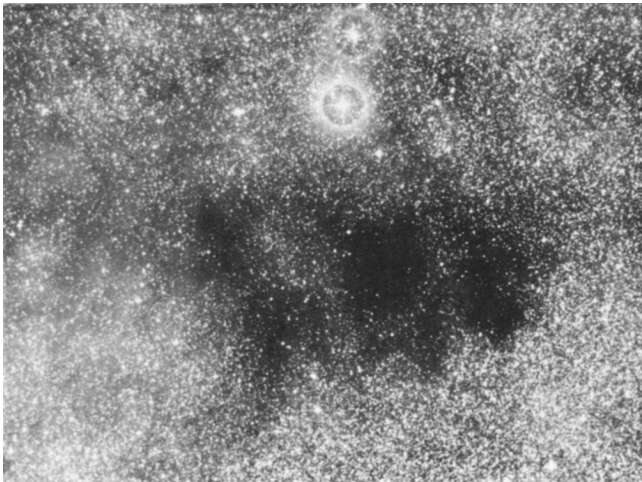


Figure 1. A positive print of the Coalsack globules 1, 2, and 3. Globule 2 is the very dense symmetrical central cloud. North is up and east to the left. The print covers an area approximately 56' x 42'. Taken from a IV N Schmidt plate courtesy of the UK Schmidt Telescope Unit.

distribution within a globule by optical means (i.e., by reddening determinations) can only be applied to the less opaque members of the class. Even the indirect star count methods run into difficulty towards the cores of the globules, as the number of observable objects tends to zero.

The advent of sensitive radio observations (particularly of the  $^{13}\text{CO}$  molecule) has revolutionised the study of globules (Martin and Barrett 1978; Dickman 1978a, 1978b). From these observations it has been possible to determine not only the mean density of the globules, but also their gas temperatures (on the order of 10 K), and an indication of their dynamical properties. In particular, the existence of suprathermal broadening of the CO lines has been interpreted in terms of velocity gradients symptomatic of collapse. Dickman (1978a) obtained similar masses for individual globules from both optical and radio techniques with the assumptions that

$$\text{CO}/\text{N}_{\text{H}_2} = 2 \times 10^{-6} \text{ and } \text{N}_{\text{H}_2}/A_V = 1.25 \times 10^{21} \text{ cm}^{-2} \text{ mag}^{-1} \quad (1)$$

(Jenkins and Savage 1974; Dickman 1978b). The latter value has been shown to be consistent for  $A_V$  up to 5 and probably as high as 10. Beyond this nothing is known. For  $^{13}\text{CO}/\text{N}_{\text{H}_2}$  however, values as low as 100 times smaller than Dickman's value have been determined in dense clouds by Wootten *et al.* (1978), by combining CO and  $\text{H}_2\text{CO}$  measurements with chemical equilibrium models. The dynamical collapse models of Villere and Black (1980) also suggest lower values of  $^{13}\text{CO}/\text{N}_{\text{H}_2}$  in regions of high density as is shown in Figure 2.

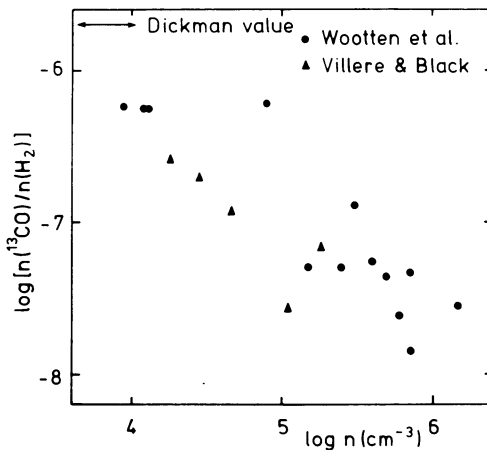


Figure 2. Relationship between the number density of  $^{13}\text{CO}$  molecules and that of molecular hydrogen ( $^{13}\text{CO}/\text{N}_{\text{H}_2}$ ), as a function of the total particle density. Filled circles are observationally deduced points from Wootten *et al.* (1978); triangles are from the best fit dynamical models of Villere and Black (1980) for well-observed globules. Dickman's (1978b) mean value for low densities is also given.

TABLE 1  
OBSERVED PARAMETERS OF SELECTED GLOBULES

Globule	Adopted Distance* (pc)	Temperature (K)	Radius (pc)	Mass ( $M_{\odot}$ )		
				Tomita et al.	Dickman	Bok et al. Others
B34	200 <sup>a</sup>		0.6	3.7 (6) <sup>†</sup>	8 <sup>d</sup>	
L134	200 <sup>a</sup>	13	0.7	41 (65)	66	280 <sup>f</sup>
B134	400 <sup>a</sup>	9	0.5	4.3 (7)	19	1 <sup>e</sup>
B335	400 <sup>b</sup>	9	0.3	3.6 (5.8)	≥23	22 <sup>f</sup> , 170 <sup>g</sup>
B361	350 <sup>a</sup>		1.0	36 (58)	17 <sup>d</sup>	86 <sup>h</sup>
Coalsack 2	175 <sup>c</sup>		0.3		25 <sup>c</sup>	11 <sup>i</sup>

NOTES: \*The mass and radii have been corrected for the distance adopted.

†Numbers in parentheses are Tomita et al.'s values adjusted upward by the factor 1.61 (see text).

- REFERENCES: <sup>a</sup>Tomita et al. 1979  
<sup>b</sup>Dickman 1978a  
<sup>c</sup>Bok 1977  
<sup>d</sup>Bok et al. 1971  
<sup>e</sup>Bok and McCarthy 1974  
<sup>f</sup>Martin and Barrett 1978  
<sup>g</sup>Villere and Black 1980  
<sup>h</sup>Schmidt 1975  
<sup>i</sup>Jones et al. 1980

1.2 Derived Globule Parameters

The crucial parameters sought in all globule studies are their total masses, radii, and temperatures. Once these are known it is possible to compare the observed position in a mass/radius diagram with predictions of the virial theorem at a given temperature. It might be expected that the observational situation in globules is clear-cut, but unfortunately, nothing could be further from the truth. It is exceedingly disconcerting to see the disparity in values of the mass for a given globule, in the published literature.

In Table 1 are collected together a sample of the derived physical characteristics of some of the best-studied globules. As one can readily see the masses obtained by different authors from similar techniques differ by factors up to 50. A detailed examination of these papers reveals that masses are obtained from visual absorption data alone in slightly different ways: see e.g. Dickman's (1978a) equation 12, Tomita *et al.*'s (1979) equation 2, and Schmidt's (1975) equation 3. These all give consistent values when applied to the same data, if Tomita *et al.*'s value of  $\alpha\delta/Q$  is adjusted upwards by a factor 1.61. Their values corrected for this factor are also given in Table 1 in brackets. While this generally improves the agreement, some cases remain widely disparate. Figure 3 presents the mass and radius values for the globules tabulated in Table 1.

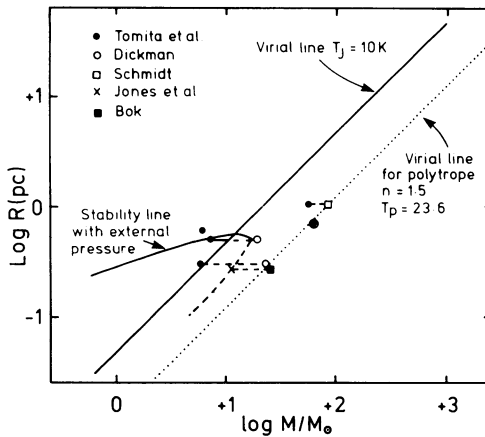


Figure 3. The mass/radius relationship for the globules listed in Table 1. Symbols are as shown in the figure. Horizontal dashed lines join globules for which two independent masses have been derived. Also shown are two virial lines (see text), and the stability line calculated by Tomita *et al.* (1979) for a 10 K sphere of gas with external pressure (see text). The solid part of the curve refers to stable equilibrium states, while the dashed portion refers to unstable equilibrium and is similar to normal virial lines.

It would appear that reliable derived masses for globules are almost nonexistent! Data in the opaque cores of the globules are of undoubted importance in resolving this issue. While several optical and near IR (Schmidt 1975; Tomita et al. 1979; Jones et al. 1980) studies suggest a plateau to the absorption in the inner regions of many globules, the data are inconclusive, and radio data suffer from a lack of spatial resolution. The dynamical collapse models on the other hand predict exceedingly dense cores and absorptions so large as to be unobservable (Villere and Black 1980), and consequently predict much higher masses than empirically determined. It would be of great interest to attempt to fit the density distribution from such models with the observations of less opaque globules.

It has been the simplistic comparison with predictions of the virial theorem which led to the conclusions that the large globules are gravitationally unstable. Figure 3 shows virial lines for  $T = 10$  K derived from

$$M/M_{\odot} = (T/0.24\mu) (R/R_{pc}) \quad (2)$$

and for a polytrope with internal pressure with  $n = 1.5$ ,  $T = 23.6$ ,  $\mu = 1$  (Kenyon and Starrfield 1979). In the standard view globules lying above the lines will continue to expand while those below are gravitationally unstable and will contract. Tomita et al. (1979) undertook a different approach in considering a mass of gas with external pressure, and have examined the conditions where  $d^2I/dt^2 < 0$ ,  $= 0$ , or  $> 0$  for  $T = 10$  K, where they have taken these to be the criteria that the object is in a state of expansion, equilibrium, or contraction respectively. Their curve for the equilibrium condition is shown in Figure 3, where the sign of  $d^2I/dt^2$  is positive and negative respectively inside and outside of the curve. According to their analysis, objects more massive than a critical value (where lines defining the stable and unstable states meet) are gravitationally unstable regardless of their radii, under the influence of external pressure.

While from their data alone it is concluded that many globules are stable configurations, the lack of consistent masses poses a great problem in the interpretation. The further derivation of stability lines for more realistic globule models will be of great value in the interpretation of new data as they become available. Certainly the belief that a large majority of these objects are unstable to gravitational contraction should perhaps be suspended until more reliable data are available.

### 1.3 An Infrared Role in the Study of Globules

1.3.1 Near infrared studies. It has been shown that optical and radio techniques for estimating the physical characteristics of globules have their limitations (e.g., opacity, resolution). The near infrared method adopted by Jones et al. (1980) essentially suffers

from neither of these problems, and offers a true direct method of deriving the density distribution within a globule. They undertook a 2- $\mu\text{m}$  survey of Globule No. 2 in the Coalsack (Tapia 1975) down to a limit of  $K \sim 9.5$  in the outer regions and  $K \sim 11.3$  in the inner  $4' \times 4'$  block. JHK photometry of each of the 75 sources discovered was then obtained and is shown in Figure 2 of their paper. It was an advantage for the object under consideration to be close to the galactic plane, since it allowed a large enough sample of background sources to be measured through the globule for determining the density distribution of the globule. From the data it is possible to derive the reddening  $E(J-K)$  on the assumption that each of the stars was spectral type M3III, a plausible assumption in terms of luminosity function calculations for the region. Figure 4 shows the derived density distribution as a function of radius from the optical center of the globule. It is clear that there is a constant background value of extinction over the whole globule which may be due to a general Coalsack sheet of obscuration, or to extinction just beyond the globule. For comparison are shown the density profiles of the modified polytropes of Kenyon and Starrfield (1979) with indices of 1.0 and 2.5. These have been claimed by Kenyon and Starrfield to fit (respectively) Schmidt's (1975) data for B361, and Bok's data for Coalsack globule 2. It is clear that the optical and near infrared data give conflicting results close to the center

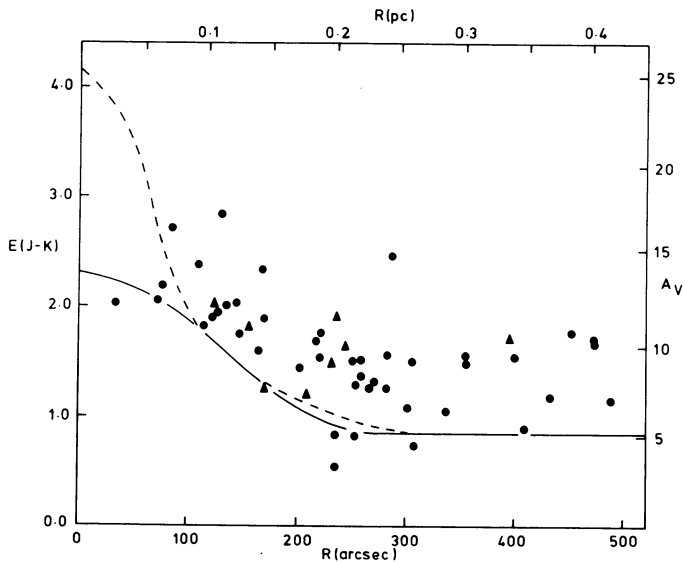


Figure 4. The color excess  $E(J-K)$  as a function of distance from the center of Coalsack globule 2, as described in the text. Filled triangles refer to stars for which spectral types had been obtained from CVF spectroscopy. The solid and dashed lines are the density profile of a polytropic model with indices  $n = 1.0$  and  $2.5$  respectively (Kenyon and Starrfield 1979) (from Jones *et al.* 1980).

of the globule. It is, however, interesting to note that in the outer parts of the globule, these data give  $\rho \propto r^{-3}$ , as did both Schmidt and Tomita *et al.*, different from the expected  $\rho \propto r^{-2}$  calculations of dynamical collapse models.

Integrating to obtain the total mass, and using the usual value  $N_{\text{H}_2}/A_V = 1.25 \times 10^{21}$ ,  $M \sim 11 M_\odot$  is derived, as shown on Figure 3. Globule 2 thus lies right on the dividing line between expansion to a stable state and gravitational contraction. Temperature measurements would be invaluable in evaluating the exact situation.

**1.3.2 Far infrared observations.** One of the most important parameters for determining the stability of globules is their temperature. Essentially all the information available has been obtained from molecular line emission (e.g., Martin and Barrett, and Dickman). An alternative approach is to search for thermal radiation from the globules, but this is difficult because of the very cool temperatures expected ( $T \sim 10$  K), and the low luminosities involved ( $L \sim 2 L_\odot$ ) if globules are externally heated by the interstellar radiation field (Werner and Salpeter 1969).

The fundamental observation of this nature is that by Keene *et al.* (1980), who obtained the far infrared and submillimeter spectrum of B335 from Mauna Kea and the Kuiper Airborne Observatory. The measurements they obtained between 150 and 450  $\mu\text{m}$  are shown in Figure 5 where they are compared with curves of the form  $B(\nu)$  (for  $T = 16$  K) and  $\nu^2 B(\nu)$  (for  $T = 13$  K), both of which give an acceptable fit to the data. The

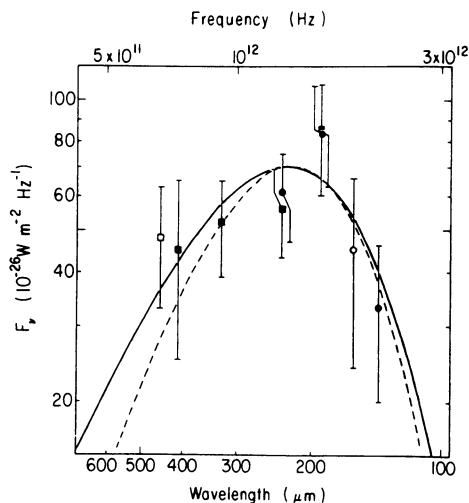


Figure 5. The observed energy distribution of B335. The solid and dashed curves have the forms  $\nu B(\nu, 16 \text{ K})$  and  $\nu^2 B(\nu, 13 \text{ K})$  respectively (from Keene *et al.* 1980).

data are also reminiscent of the silicate ice model energy distributions given by Spencer and Leung (1978).

The main conclusions of Keene *et al.* (1980) may be summarized as follows:

- a) radiation from the globule with a luminosity of  $\sim 5 L_{\odot}$  (at 400 pc) is optically thin thermal emission,  $\tau_{225} \sim 0.010$  with  $T$  lying in the range 13–16 K.
- b) the dust mass lies between  $0.07 M_{\odot}$  and  $0.17 M_{\odot}$  in agreement with values given in Table 1 for a gas/dust ratio of  $\sim 100$ .

Keene *et al.* show that it is unnecessary to invoke the presence of an internal luminosity source within the globule as heating by the interstellar radiation field (particularly if modified in the manner of Jura [1979]) is by far the most important source of heating. It would appear from this first far infrared approach that the physical parameters of B335 are firmly established, and that they all consistently suggest that B335 is gravitationally bound.

The aim in this discussion has been to show that infrared observations at both short and long wavelengths have a vital role to play, in producing a clear picture of the structure and physical processes involved in the formation and evolution of globules. Probably the most puzzling aspect of the study of Bok globules, and the question with which I would like to complete the discussion, is what is the next phase of evolution, and do we see it? Why is it, for instance, that we do not appear to see globules with a wide variety of radii and similar masses? After all, they are expected to evolve downwards in the mass-radius diagram (Figure 3) yet no high-mass small-radii globules appear to have been observed. This perplexing question suggests two perhaps heretical alternatives: (a) our techniques are not sufficiently refined to obtain the parameters of such objects should they exist, or (b) globules are intrinsically stable, and have nothing to do with star formation.

## 2. DARK CLOUD REGIONS OF LOW MASS STAR FORMATION

### 2.1 Introduction

In this section of the paper I shall give an overview of infrared work on nearby dark cloud complexes and, in section 3, will discuss the IR characteristics of PMS objects.

It is my object to concentrate on those dark cloud regions where low mass ( $1-2 M_{\odot}$ ) star formation is occurring and where violent processes do not appear to be dominant. Associated with these are the well-known emission line T Tauri stars, initially recognized as a class by Joy (1945). It is now universally accepted that T Tauri stars, and associated objects embedded within the dark cloud complexes, are low mass pre-main sequence objects.

Detailed optical studies of dark cloud regions have been hampered by obscuration within the clouds. In the last decade, however, infrared observations have made tremendous strides in penetrating the veil of these clouds, which has in turn led to a much better understanding of the population of newly formed stars enshrouded within them.

## 2.2 Near Infrared Surveys of Dark Cloud Regions

**2.2.1 Historical background.** The fundamental and pioneering set of near infrared observations was a 2  $\mu\text{m}$  survey of part of the  $\rho$  Ophiuchus dark cloud by Grasdalen *et al.* (1973) which was extended by Vrba *et al.* (1975). Their work revealed for the first time a group of obscured embedded sources near the center of the cloud, which they interpreted as members of an embedded young cluster within the cloud, the possible existence of which had been suggested more than a decade previously (Bok 1956). Spurred on by this success, this group of workers undertook a series of comprehensive 2  $\mu\text{m}$  surveys in a variety of dark cloud regions, and combined these with optical spectroscopy and photometry (K. Strom *et al.* 1975, 1976; S. Strom *et al.* 1976; Vrba *et al.* 1976). In parallel with this undertaking, Rydgren *et al.* (1976) published a major study of the properties of optical T Tauri stars, and S. Strom *et al.* (1974) investigated in detail the properties of the related Herbig-Haro objects (Herbig 1969). Many of the conclusions of these studies have been summarized in two review papers by S. Strom *et al.* (1975) and S. Strom (1977).

Following the success of the initial study of  $\rho$  Oph, it was disappointing to find that in many regions (e.g., L1630, L1517, R CrA) the obscured cluster hypothesis was not viable. Although a number of 2  $\mu\text{m}$  sources were found in each survey (some undoubtedly associated with the dark cloud complex) no further major population of PMS objects was found. In particular, study of the nearby R CrA region provided no evidence for an embedded cluster (Vrba *et al.* 1976) despite the overwhelming evidence of recent star formation in the region (Knacke *et al.* 1973; Glass and Penston 1975).

The one major criticism which can be levelled at the interpretation of the early surveys was the failure to take careful account of confusion by background sources. Although several of the regions investigated lie well above the plane, the general galactic background of old disk stars is still significant. For example at the position of  $\rho$  Oph, in a region covering 0.2 square degrees, and down to a K magnitude of 10, one expects (from a simple luminosity function and exponential disk model of the galaxy) to find 41 background sources! This is well over half the number of sources found in the survey of Vrba *et al.* (1975) and has profound consequences on any conclusions from that survey.

**2.2.2 Taurus, Ophiuchus, and the background sources at 2  $\mu\text{m}$ .** The first person to realize the importance of the background contribution to 2  $\mu\text{m}$  survey material was Elias (1978a,b,c) in his studies of IC 5146, and the Ophiuchus and Taurus dark clouds. In the latter two cases,

Elias undertook massive surveys, covering respectively 18 and 20 square degrees, and detecting some 400 and 200 stars respectively down to a K magnitude of +7.5. Examination of his Figure 1b (Elias 1978b,c) shows clearly that the sources were essentially evenly distributed over both clouds, and it was therefore essential to distinguish between objects within the cloud and background field stars. This was undertaken first by restricting the sample to objects with  $H-K \geq 0.70$  and  $K < 7.0$ . Elias then undertook the daunting task of obtaining CVF spectroscopy and broad band colors for the selected sources, and used the spectroscopic data to identify the sources associated with the cloud. Figure 6 shows the 2–2.5  $\mu\text{m}$  spectra obtained by Elias (1978c) in Taurus. The basis for the identification is that according to the model of the galactic stellar distribution (Elias 1978a), almost all the field stars should be G8 giants and later, and identifiable by their CO absorption beyond 2.3  $\mu\text{m}$ . The association objects, however, are likely to have smooth energy distributions either as a result of their earlier spectral type, or as a result of excess thermal or gaseous emission in the 2  $\mu\text{m}$  region.

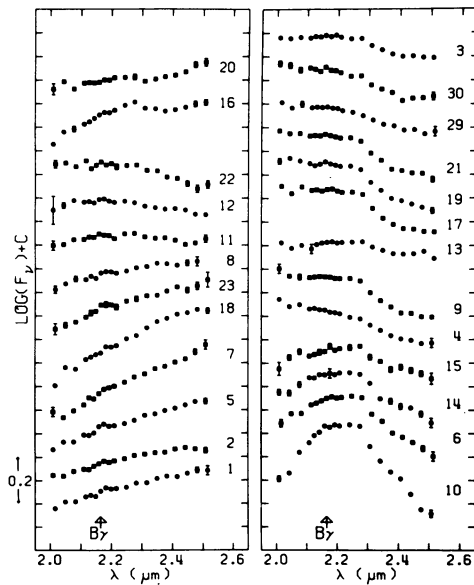


Figure 6. 2  $\mu\text{m}$  spectra of selected objects in the Taurus dark cloud complex. All the objects in the right half of the figure plus Nos. 16 and 20 have been classified as background field stars (from Elias 1978c).

As an example of the photometric properties of the embedded sources, Figure 7 shows photometry of the Oph sources by Elias (1978b). It can be seen that these objects exhibit a wide variety of characteristics, the common feature being that most exhibit some kind of infrared excess. By examining background objects, Elias concluded that the infrared reddening law in Taurus and Ophiuchus was identical and the same as the normal interstellar law. Of particular interest are the 3 objects shown at the right of Figure 7. All 3 of these are extremely red objects, appear extended at  $1.6 \mu\text{m}$ , and are interpreted by Elias as obscured reflection nebulae formed within regions where the minimum molecular hydrogen density is  $10^5$  molecules  $\text{cm}^{-3}$ . Both polarization measurements and high resolution maps at  $1.6$  and  $2.2 \mu\text{m}$  are needed to elucidate the properties of these interesting objects further.

There is an alternative method of determining the membership of PMS sources within a cloud which is almost 100% effective, i.e., their position in a JHK diagram. This technique, being significantly faster than CVF spectroscopy, would have enabled Elias to enlarge his sample of sources dramatically. Figure 8 shows a plot of his JHK photometry in a J-H vs H-K diagram for both Ophiuchus (right) and Taurus (left). The association and field stars as identified by Elias are plotted as different symbols. Almost all the association objects can be easily identified by their (H-K) excesses, and certainly none of the Taurus field stars (apart from the peculiar variable RV Tauri) fall in that part of the diagram. They follow a remarkably tight locus in the diagram for which as yet no satisfactory explanation has been advanced, although it is probably tied up with the nature and evolution of the circumstellar shells, which are one explanation for the infrared colors of PMS objects (see 3.1).

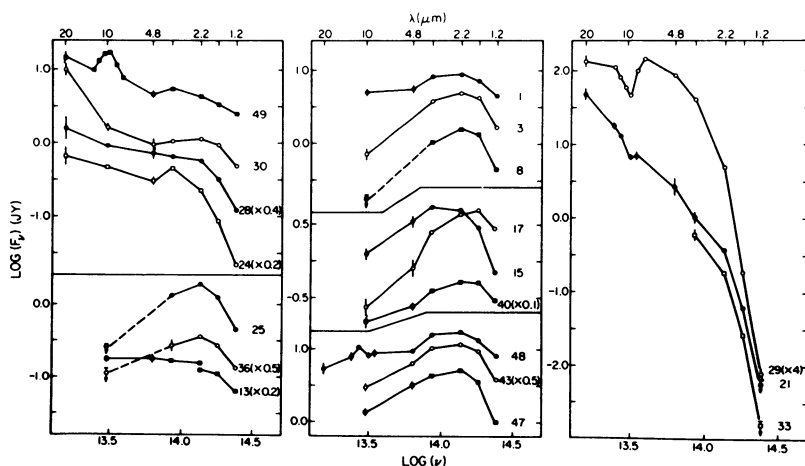


Figure 7. Energy distributions of selected objects in the  $\rho$  Oph dark cloud between 1 and  $20 \mu\text{m}$  (from Elias 1978b).

The work of Elias showed that there are clear differences between Ophiuchus and Taurus, which are apparent in the embedded population as well as in the optical stars. The exact reasons for these differences obviously lie in the obscure details of the star formation triggering process (see 2.3). It is unfortunate that these surveys did not go to fainter magnitudes, especially in Taurus, as the presence in large numbers of low luminosity embedded sources and their spatial distribution might substantially alter current thinking on star formation within that cloud.

2.2.3 Studies of the Chamaeleon dark cloud complex. The Chamaeleon T association was first recognized by Henize (1963) and Hoffmeister (1962) and consists of an elongated dust cloud containing a large sample of emission line stars and three conspicuous reflection nebulae. Henize and Mendoza (1973) discussed the spectra of some 32 emission line stars within the association, while subsequently Feast and Glass (1973) showed one to be an R Mon type object, Schwartz (1977) discovered several Herbig-Haro objects in the cloud, and Appenzeller (1977, 1979) reported a high percentage of YY Ori type spectra among the emission line stars. In all ways, Chamaeleon is an ideal region for the detailed study of low mass PMS objects and their interaction with their placental dark cloud: it is close ( $\leq 200$  pc), is substantially out of the galactic plane ( $b \sim -15^\circ$ ) and contains a significant population of young objects.

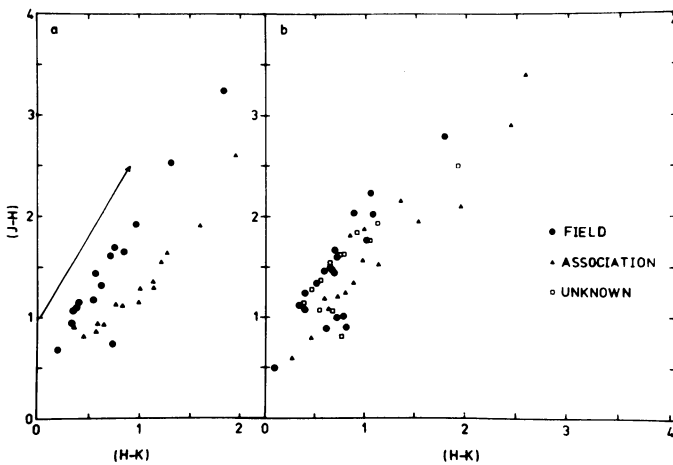


Figure 8.  $(J-H)$  vs  $(H-K)$  diagrams for the objects measured by Elias (1978b,c) in  $\rho$  Oph (right) and Taurus (left). Filled circles and filled triangles refer to field and association stars defined by Elias on the basis of spectroscopy. Open squares are objects for which there is no spectroscopic data. The association objects are separated very clearly by an excess  $E(H-K)$  in this diagram.

Grasdalen *et al.* (1975) and more recently Rydgren (1980) obtained photometry and spectra of the emission line objects, and derive different distances to the association on the basis of an anomalous reddening law within the cloud ( $R = 5.5$  and  $5.0$  respectively). Glass (1979) obtained JHKL photometry of almost all the HM emission line stars, as well as a selection of apparently background objects. The latter appeared to follow a normal interstellar reddening curve well (in the near infrared), while the emission line objects occupied a similar locus in (J-H) vs (H-K) diagram as the T Tauri stars in Taurus (Figure 8).

Hyland and Jones (1980) have undertaken a systematic  $2 \mu\text{m}$  survey and follow-up observations to search for previously unrecognized embedded PMS objects, and to map the interstellar reddening through the cloud by observations of the background stellar population. The area covered in the initial phase of this survey was approximately  $0.32$  square degrees; the (J-H) vs (H-K) diagram for the sources discovered is shown in Figure 9.

Several interesting features may be noted in Figure 9: (a) the "background" sources follow the normal interstellar reddening curve in the near infrared (Jones and Hyland 1980); (b) the embedded sources follow the locus of similar objects in Taurus, and include several objects which were too faint to be recognized in optical surveys; (c) there is a large group of stars clustered in the region (J-H)  $\sim 0.6$  (H-K)  $\sim 0.3$  which are absent from the similar figure for background objects in the Coalsack region. Spectroscopic observations of several of these (Schwarz 1977; Hyland and Jones 1980) reveal weak Balmer emission, suggesting that these may be a population of less extreme PMS objects lying closer to the main sequence. If so, the population of PMS objects within Chamaeleon, including the newly found obscured sources, may need to be increased by as much as a factor of two over the number of optically discovered emission line stars.

It is evident that the intrinsic (i.e., reddening-free) colors of the embedded sources are greatly influenced by extinction within the cloud and it is necessary to devise a means of taking this into account. Figure 10 is a map of the positions of background stars and embedded (IR excess) sources found in the survey. With the assumption that the mean spectral type of the background sources is K1 III (as predicted by a simple exponential disk model of the galaxy in the manner of Elias 1978a), values of  $E(J-K)$  and  $A_V = 5.6 E(J-K)$  were obtained. These were then combined to form the approximate contour map shown in Figure 11, which can be used to obtain upper limits to the effect of cloud extinction on the colors of the embedded sources.

Figure 11 also provides an interesting and unexpected insight into the spatial distribution of the young embedded sources within the cloud. There is clearly a small grouping of PMS objects at the position  $11^{\text{h}}08^{\text{m}}30^{\text{s}}$ ,  $-76^{\circ}19'$ , right at a steep density gradient. The triangle indicates the position of the Be star HD 97300 which illuminates the

bright reflection nebula. This clustering is highly suggestive that the more massive early-type star has caused compression of the gas in its neighborhood, creating the conditions for and triggering further star formation. While it is less apparent in the data presently available, there is a similar group of embedded sources at  $11^{\text{h}}07^{\text{m}}$ ,  $-77^{\circ}29'$ , which also lie on the boundary of the possible interaction of HD 97048 with the dense cloud material.

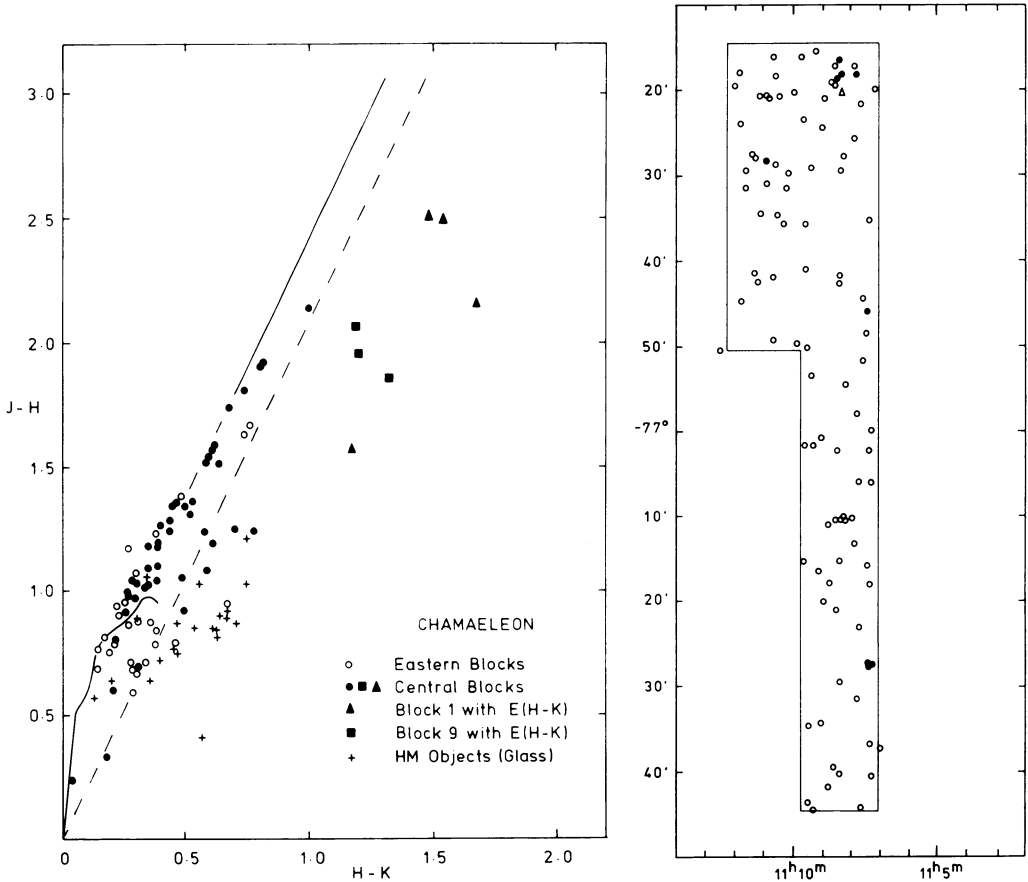


Figure 9 (left). (J-H) vs (H-K) for the objects in Chamaeleon revealed by the  $2 \mu\text{m}$  survey (Hyland and Jones 1980), plus the Henize and Mendoza objects measured by Glass (1979) which lie outside the survey region. Objects with extreme excesses E(H-K) are shown as filled triangles and filled squares.

Figure 10 (right). The distribution of objects found in the  $2 \mu\text{m}$  survey in Chamaeleon. Filled symbols refer to objects with extreme excesses of E(H-K).

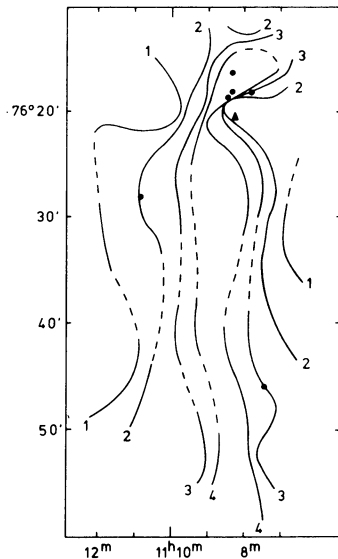


Figure 11. Map of the distribution of reddening  $E(J-K)$  in the northern region of the Chamaeleon  $2 \mu\text{m}$  survey, derived from background field stars. The filled circles refer to objects with extreme  $E(H-K)$  excesses. The contours refer to the following values of  $E(J-K)$ : #1 =  $\leq 0.40$ , #2 = 0.65, #3 = 0.90, #4 =  $\geq 1.15$ .

Deep  $2 \mu\text{m}$  surveys when combined with photometry and optical data appear to provide an extremely powerful probe of dark cloud regions, which, despite all the work which has so far been undertaken, has yet to realize its full potential.

### 2.3 Spatial Clustering and Triggering Mechanisms in Low Mass Star Formation Regions

The idea of sequential star formation has been advanced to explain the nature of OB associations (Elmegreen and Lada 1977). In their model, ionization-driven shock fronts from an initial group of OB stars propagate into a dense molecular cloud; eventually the gas which has accumulated between the shock and ionization fronts becomes gravitationally unstable, initiating the formation of OB stars. While this picture has been eminently successful in delineating high mass star formation processes in giant molecular clouds, the picture in dark clouds associated with low mass ( $M \sim 1 M_{\odot}$ ) star formation is unclear. In these there is no obvious population of first generation objects with high enough stellar winds to compress the interstellar gas, and the spatial distribution of optical T Tauris is generally fairly even over the cloud's extent (although embedded sources may have been missed). There is, however, some information on clustering of PMS objects and triggering mechanisms within such clouds, which may throw some light on the processes of star formation in them.

1. The infrared observations of Elias (1978b) where background objects have been eliminated provides evidence on the presence of a considerable embedded cluster of stars at the center of the  $\rho$  Oph cloud. This is the only cloud for which an extensive cluster has yet been identified.

2. IC 5146 (Elias 1978a) is similar in many respects to  $\rho$  Oph, although many of the cluster stars have already reached the main sequence. The spectral type of its earliest star is BOV. From CO observations which show several intense bright spots, Lada and Elmegreen (1979) have found evidence for clustering of star formation within the cloud complex. They suggest that star formation of stars with spectral type later than B is occurring and "has been most intense in a small ( $\sim 5$  pc), dense, possibly compressed molecular core located at one end of the more extended ( $\sim 20$  pc) cloud complex."

3. Elias (1979c) finds no evidence for widespread clustering within the Taurus cloud (though it should be remembered that his survey was not very deep), but there are small clusterings of young objects. L 1551 is a case in point where two visible T Tauri stars (HL and XZ Tau), 3 Herbig-Haro objects, and an embedded infrared source are found in close proximity. Fridlund et al. (1980) have recently made balloon-borne far infrared observations of the region, and identify a 65  $L_{\odot}$  point source with the embedded source (IRS 1). They conclude that it too is T Tauri in nature.

4. Evidence for small scale clustering of PMS objects in Chamaeleon (Hyland and Jones 1980) has already been mentioned (2.2.3). Further observations to complete the whole cloud are required to examine the overall picture.

5. CO observations of the R CrA region (Loren 1979) show the greatest heating of the CO occurs in the regions close to the B star TY CrA and the PMS object R CrA. The population of embedded objects so far discovered is extremely small, and the CO observations further imply a nonhomologous collapse of the core of the molecular cloud, while the cloud is also elongated at all densities up to  $4 \times 10^5 \text{cm}^{-3}$ .

While these data provide some evidence on star formation mechanisms in dark cloud regions, there is no coherent picture regarding triggering mechanisms, and it may be that there are as many mechanisms as there are clouds to contemplate. For example, in  $\rho$  Oph, Vrba (1977) has argued that the magnetic field geometry and spatial distribution of some of the youngest stars is indicative of external shock compression. Elias (1978c) points out that some of the embedded objects may postdate the age given to the initial shock compression ( $\sim 6 \times 10^6$  yrs) and speculates that an event such as a supernova (Herbst and Assousa 1977) which produced the runaway  $\zeta$  Oph may also have triggered the most recent star formation.

In Taurus, Elias (1978c) suggests that star formation has been spontaneous, notwithstanding the small scale clustering mentioned earlier. In R CrA, Loren (1979) interprets the lack of CO line splitting in the denser star formation regions of the cloud as conclusive evidence that dynamical effects can be ruled out. He suggests that Vrba's (1976) hypothesis that the evolution of the cloud is controlled by flow along magnetic field lines is correct, and indicates

that star formation should and does occur in the region of the cloud closest to the galactic plane. On the other hand, IC 5146 resembles  $\rho$  Oph and M17 where regions of active star formation are located in the dense tips of elongated molecular clouds at the end furthest from the galactic plane. Lada and Elmegreen (1979) suggest externally applied pressure as the trigger in all three cases.

The picture of triggering mechanisms for regions of low mass star formation is thus in a state of great flux and is very much a problem for the 1980s.

#### 2.4 The Reddening Law in Dark Cloud Regions

A knowledge of the extinction law in dark clouds is of crucial importance for determining the intrinsic energy distributions and luminosities of the sources within the clouds. Furthermore, the derived distances to many clouds depend critically upon the value of  $R$  [ $A_V/E(B-V)$ ] used to deredden the photometry of the stars. It has long been suggested on the basis of optical photometry (e.g., Walraven and Walraven 1960; Hardie and Crawford 1961) that values of  $R$  considerably greater than the normal interstellar value may exist. Carrasco *et al.* (1973) produced evidence from optical and infrared photometry for a wide variety of  $R$  values (ranging from 3 to 5) within the Ophiuchus dark cloud complex, and showed that  $R$  increased with the total extinction. They concluded from their observations that "the mean particle size increases in the denser parts of the Rho Oph cloud." It is certainly not clear to what extent the large values of  $R$  adduced from deeply embedded stars can be applied to other objects within the cloud, yet this procedure has been adopted in certain cases with possible misleading results. Cohen and Kuhl (1979) have argued strongly against this kind of approach, and advance good arguments for rejecting large values of  $R$  for the less embedded optical T Tauri stars in Taurus and Ophiuchus.

Grasdalen *et al.* (1975) derived  $R = 5.5$  from optical and near infrared observations of HD 97300, the AOV illuminating star of Cederblad 112 in the Chamaeleon region. Using this value to derive the distance to the cloud forced many of the young emission line T Tauri stars to fall below the zero age main sequence. More recent observations by Rydgren (1980) suggest a marginally smaller value of  $R = 5.0$ , but even he cautions against blind adoption of this value, since both stars used in the derivation are probably very young and may have weak circumstellar dust shells.

The problem with all determinations of the reddening law in dark cloud regions discussed earlier is that they have been obtained from observations of young stars intimately associated with or deeply embedded within the clouds. These are just those stars which might be expected to possess extensive circumstellar dust shells as probable remnants of their recent protostellar phase of evolution, and we will see in fact that many do so. However, a number of authors (Elias 1978a,b; Glass and Penston 1975; Glass 1979; Jones and Hyland 1980; and

Jones *et al.* 1980) have observed background field stars seen through the Taurus, Ophiuchus, R CrA, Chamaeleon, and Coalsack clouds, and have shown that the reddening law in the near infrared is normal. They also show that embedded objects generally have infrared excesses consistent with the presence of circumstellar shells (see 2.2.3). Unfortunately, none of the reddening determinations of background stars have been tied to optical photometry, and in the most opaque regions of the clouds it is unlikely that such observations will ever be attempted.

However, although the mean infrared extinction law appears to be unchanged within dark cloud regions, this does not preclude a change in the reddening law at shorter wavelengths. Some exciting new results obtained from near infrared photometry of O stars in the Carina nebula by Smith (1980) are particularly relevant. A combination of the new infrared data with the optical results of Feinstein *et al.* (1973) gives unequivocal evidence for an anomalous reddening law, with a unique value of  $R = 5$ . Interestingly, the data can be interpreted in terms of a change in the absorption characteristics of the grains in the B filter pass band alone. Thus, for objects which appear to follow the normal reddening law in the near infrared, it is probably safer to derive  $A_V$  from the normal value of  $A_V/E(V-K)$ , and to disregard B entirely. Clearly, however, no definitive statement on the interstellar reddening law in dark clouds can be made at this time, and it remains one of the most pressing problems within the larger context of dark clouds and star formation.

### 3. THE INFRARED CHARACTERISTICS OF PMS SOURCES

#### 3.1 Nature of Near IR Continua

T Tauri stars have been noted for their large infrared excesses since the early work of Mendoza (1966, 1968). As each new group of T Tauris and embedded PMS stars has been observed, more sources with large infrared excesses have been found (e.g., Cohen 1973a,b; Vrba *et al.* 1975; Knacke *et al.* 1973; Grasdalen *et al.* 1975; Glass 1979). While initial interpretation of these was made in terms of thermal emission from circumstellar dust, the striking emission lines in the optical spectra of T Tauri stars led Grasdalen *et al.* (1975) to propose free-free emission from a hot ( $T \sim 2 \times 10^4$ ) gaseous envelope as the major mechanism producing the infrared continuum (see also S. Strom 1977)

The ability to distinguish between the two proposed mechanisms is in no small measure dependent upon obtaining the correct reddening law to use. In particular, at J, H, and K, reddening within the clouds may be substantial, and is of great importance for determining the "intrinsic" (i.e., reddening-free) position of individual stars in the (J-H) vs (H-K) diagram. Any means whereby the total cloud reddening can be mapped, e.g., optical star counts, using background objects as outlined in 2.2.3, or from  $^{13}\text{CO}$  measurements, will prove invaluable in setting upper limits to the cloud contribution to the stellar colors.

Also, it is possible with little error to deredden at infrared wavelengths, since the ratios  $E(J-H)/E(H-K)$ , etc., have been directly determined by reference to background objects.

Rydgren (1976) computed (J-H) vs (H-K) diagrams for models incorporating a stellar photosphere plus free-free and free-bound emission from a hot gaseous envelope to interpret the colors of T Tauri stars and to separate interstellar reddening from the gaseous component. Baschek and Wehrse (1977) pointed out that the inclusion of line emission would reduce the effect of the envelope emission on the colors. Rydgren (1976) and Strom (1977) consider the inphase variation of optical and infrared brightness a strong argument in favor of the gaseous envelope model. However, it now appears that while such a model might be the explanation for the colors of some T Tauri and PMS objects, there are many whose extreme colors require an alternative explanation, presumably in terms of hot circumstellar dust.

Cohen and Kuhi (1979) have undertaken the most recent thorough examination of this question and clearly favor the hypothesis of thermal emission from dust for the large majority of T Tauri stars. Their Taurus-Auriga observations in a (1.6-2.3) vs (2.3-3.5) diagram [(H-K) vs (K-L)], corrected for interstellar reddening, are shown in Figure 12. Thermal excesses are emphasized in such a figure compared with shorter wavelength data. It is clear that although a number of the objects lie close to the photosphere + hot-gas-emission line, the majority have even larger excesses and require thermal emission to be present. Cohen and Kuhi also claim that lack of an observed emission Balmer jump, in contrast to the predictions of the envelope models, strongly suggests that the infrared excess does not arise from gaseous emission.

One important conclusion of the thermal emission hypothesis demanded by JHKL magnitudes is that there is a predominance of hot grains ( $T \sim 1500$  K) in the circumstellar shells, suggesting either that the inner boundary of the shell is very close to the star, or that mechanical heating is important. Furthermore, the grain mix must be such that it contains a sizeable percentage of refractory grains such as graphite. Some objects (e.g., T Tau) show strong evidence for cool ( $T < 500$  K) emission and many have excesses out to  $20 \mu\text{m}$  (Cohen 1973a,b). It is probable that the considerable differences between the characteristic energy distributions of PMS stars and those of late type giants with mass loss nebulae reflects a fundamental difference in the nature and history of their circumstellar shells.

### 3.2 Far Infrared Observations

Probably the most exciting advance in the last year in the understanding of young emission line PMS stars and their relationship to remnant protostellar material has been the far infrared study of young emission line objects by Harvey *et al.* (1979), in which 50 and 100  $\mu\text{m}$  observations of 8 young emission line stars (including two classical T Tauri stars) were obtained. The spectral energy distributions of these objects from 1 to 100  $\mu\text{m}$  are shown in Figure 13. The remarkable

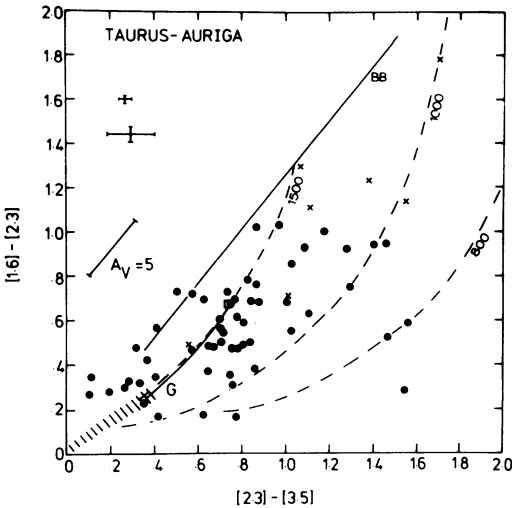
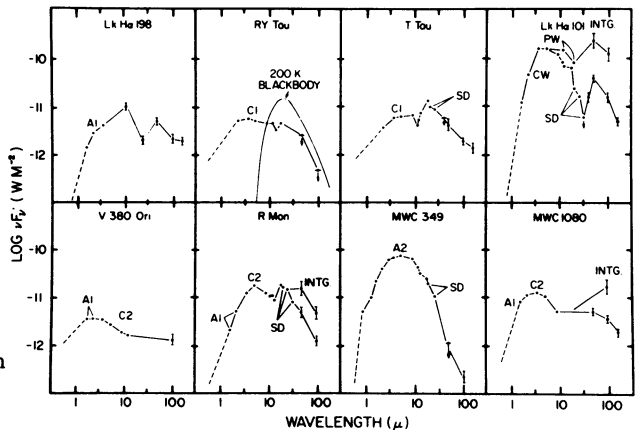


Figure 12. Intrinsic 2 color near IR plot for stars in the Taurus-Auriga clouds. Filled circles refer to stars for which a continuum extinction can be determined; crosses refer to continuum stars for which observed rather than intrinsic colors are plotted. 1  $\sigma$  error bars are shown for the brighter and more typical stars. The hatched area represents the locus of main-sequence stars. The solid line (BB) represents the locus of blackbodies. The solid curve (G) terminated by an open square indicates the locus of a K7 photosphere with increasing superposed optically thin free-free, free-bound, and bound-bound gas continuum emission. The dashed lines refer to a K7 photosphere overlaid by thermal emission from hot dust grains at 800, 1000, and 1500 K (from Cohen and Kuhi 1979).

feature of these data is the extremely broad energy distribution and unexpected strong far infrared emission. Harvey *et al.* (1979) interpret these observations in terms of very extensive circumstellar dust shells with optical depths  $\tau \sim 0.01$  at 100  $\mu\text{m}$ , implying  $\tau \leq 1$  at visual wavelengths. It is necessary to invoke a slow radial dependence of dust density ( $\rho \propto r^{-1}$ ), high maximum temperatures for the inner regions of the shell, and very cool minimum temperatures at the outermost regions of the shell ( $T \leq 20$  K), to model in a simplistic way the flat type of

Figure 13. Energy distributions of 8 emission line stars discussed by Harvey *et al.* (1979). Total integrated far infrared fluxes are given for the extended sources associated with Lk H $\alpha$  101, R Mon, and MWC 1080. A 200 K blackbody spectrum is also shown on the RY Tau graph to illustrate the fact that many of the stellar energy distributions are much broader than that of a single-temperature blackbody (from Harvey *et al.* 1979).



the shell, and very cool minimum temperatures at the outermost regions of the shell  $T \leq 20$  K, to model in a simplistic way the flat type of energy distribution. The observations thus set strong constraints on any circumstellar dust shell model for T Tauri energy distributions.

The extensive nature of the shells is further emphasized by the observation that two of the sources are resolved at  $100 \mu\text{m}$ , and have typical sizes  $\sim 50\text{--}60''$ . In physical terms the outer radii of the shells range from  $\sim 10^{16}$  to  $10^{18}$  cm which, although large, are clearly small compared with the overall dark cloud dimensions. The  $r^{-1}$  dependence of dust density suggests strongly that the shells are remnants of the protostellar clouds from which the objects were formed, and is unlike normal mass loss nebulae (where  $\rho \propto r^{-2}$ ).

These observations suggest that a systematic study of far infrared emission from a wide range of obscured PMS and optical T Tauri stars may be expected to provide important new clues on the development of remnant protostellar clouds with age.

### 3.3 Infrared Spectroscopy

The CVF ( $\lambda/\Delta\lambda \sim 100$ ) observations of Cohen (1975) covering  $2\text{--}4 \mu\text{m}$ , and similar ( $2\text{--}2.5 \mu\text{m}$ ) observations of the Taurus and Ophiuchus sources by Elias (1978a,b), are the only substantial spectroscopic contributions beyond  $1 \mu\text{m}$  to the present time. Hyland and Jones (1980) have obtained a number of  $2\text{--}2.5 \mu\text{m}$  spectra of embedded Chamaeleon and R CrA sources, while Mould and Ridgway (1980) have recently obtained high-resolution ( $1 \text{cm}^{-1}$ ) data for some 7 T Tauri stars.

All these observations confirm the generally smooth infrared continua in the  $2\text{--}4 \mu\text{m}$  range (see Figure 6), reminiscent of smooth dust continua. The new high-resolution data reveal for the first time the weak emission features  $\text{Br}_\gamma$  and  $4733 \text{cm}^{-1}$  (a possible line of He I) in several of the sources. It will be possible to use the strength of  $\text{Br}_\gamma$  in conjunction with optical emission lines to place further constraints on the importance of gaseous emission in the near infrared. Cohen (1975) found a measurable  $3.1 \mu\text{m}$  ice absorption feature in only 1 of 21 objects observed (HL Tau), and a weak  $3.3 \mu\text{m}$  emission feature in Lk H $\alpha$  - 198. Blades and Whittet (1980) have recently found a striking unidentified emission feature at  $\sim 3.5 \mu\text{m}$  in the spectrum of the Chamaeleon PMS star HD 97048, which clearly originates in the star's own circumstellar shell. Beckwith *et al.* (1978) searched for  $\text{H}_2$  emission in T Tauris, the only positive detection being T Tauri itself.

Definitive evidence on the nature of the circumstellar dust material around PMS stars comes only from the narrow band photometry and CVF spectroscopy in the  $8\text{--}14 \mu\text{m}$  region (Cohen 1980; Rydgren *et al.* 1976). Figure 14 shows three examples of silicate emission from PMS stars taken from the work of Cohen. These show similar features which match well with the Trapezium-like grains for temperatures between 200 and 300 K. Of the stars so far observed, only HL Tauri shows evidence for interstellar silicate absorption.

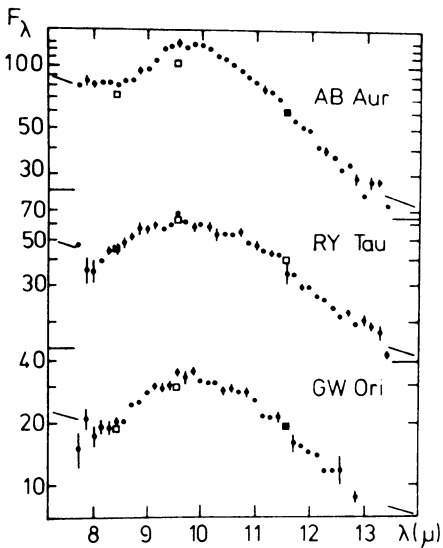


Figure 14. Observed spectrophotometry of 3 T Tauri stars. Open squares indicate independent bound-bound flux calibrations. Tick marks at the edges of the spectra indicate the interpolated linear continua used to define  $10 \mu\text{m}$  features. Where plottable,  $1 \sigma$  photometric errors are shown at each wavelength. Units of  $F_\lambda$  are  $10^{-18} \text{ W cm}^{-2} \mu\text{m}^{-1}$  (from Cohen 1980).

### 3.4 Age and Evolutionary Status of PMS Objects

Among the important parameters which one would like to determine for the PMS stars are their masses, radii, ages, and hence the age spread and mass function within a given association. This can at the present time only be done for optically observable PMS objects, and even then the systematic errors leave one in doubt as to the true value of any such approach. The placement of such objects accurately within an HR diagram depends upon: the accuracy with which the spectrum can be determined (given the problems of emission lines extending into the spectrum), the distance to the cloud (and its dependence on  $R$ ), and the bolometric correction taking into account all infrared and UV radiation. These then need to be compared with appropriate theoretical evolutionary tracks; Cohen and Kuhi (1979) have made the most systematic attempt so far to use this technique. They used a variety of sources to obtain consistent convective-radiative tracks with which to compare the observations, since the dynamical evolutionary tracks of Larson (1972) predict no visible objects in the region of the HR diagram occupied by PMS objects. Their Figures 2 and 6 show HR diagrams for PMS stars in Taurus and Ophiuchus compared with the theoretical tracks, while their Figure 7 shows the theoretical tracks with isochrones added.

It is immediately apparent that there is a wide age spread in each of the clouds examined, although the mean age for both Taurus and Ophiuchus is around  $8 \times 10^5$  years. Furthermore, the "growth" parameter of Cohen and Kuhi (1979), which is a timescale for increasing the visible stellar population by a factor of 10, is almost the same for Taurus and Ophiuchus. It would appear that the differences between the two groups mentioned earlier cannot be attributed to age. It is unfortunate that the mass spectrum for Ophiuchus is too sparse for comparison with that

of Taurus, although on the surface it would appear that Taurus has a relatively larger population of  $0.8\text{--}1.0 M_{\odot}$  objects.

#### 4. CONCLUSION

It is unfortunate that, due to limitations of space, many topics have only been covered in the briefest manner, and some important areas, such as the efficiency of star formation, have been omitted. In particular, the efficiency of star formation, which varies widely from cloud to cloud, is of great interest in delineating differences between regions, and Vrba (1977) has postulated that the efficiency directly relates to the detailed dynamical processes which trigger star formation, and to the strength of magnetic fields which may conspire to prevent or delay collapse of the clouds.

The role of infrared observations in the advancement of our insight into such processes has never been greater, and is in a state of continued expansion. It will be apparent from the foregoing discussion that there are not only significant gaps in our knowledge of these processes but that the basic parameters on which our understanding is based leave much to be desired. One of our major blind spots appears to be a coherent picture of the triggering of low mass star formation and the effects of magnetic fields within the clouds. Clearly infrared polarization measurements will play an increasing role in the understanding of field geometry and its relationship to collapse prevention.

High-resolution spectroscopy, increased molecular mapping, and the mass of mid and far infrared data expected from IRAS will undoubtedly spark major new analyses of the temperature, density, and velocity structure of dark cloud regions. The results of these and follow-up observations from SIRTf should contribute greatly to our understanding of the differences and similarities of these complexes.

In addition to these observational approaches, the time is now ripe for improved models for the photospheres and circumstellar shells of PMS objects, and for a search for dynamical collapse models which satisfy the present observations of pre-main-sequence evolution. With the wealth of opportunities now available to advance the field significantly, it is clear that globules, dark clouds, and PMS objects are going to provide good hunting for observer and theoretician alike in the coming decade.

#### REFERENCES

- Appenzeller, I.: 1977, *Astron. Astrophys.* 61, pp. 21-26.  
Appenzeller, I.: 1979, *Astron. Astrophys.* 71, pp. 305-309.  
Baschek, B., and Wehrse, R.: 1977, *Publ. Astron. Soc. Pacific* 89, pp. 345-346.

- Beckwith, S., Gatley, I., Matthews, K., and Neugebauer, G.: 1978, *Astrophys. J. Letters* 223, pp. L41-L43.
- Blades, C.J., and Whittet, D.C.B.: 1980, *Monthly Notices Roy. Astron. Soc.* 191, pp. 701-709.
- Bok, B.J.: 1956, *Astron. J.* 61, pp. 309-316.
- Bok, B.J.: 1977, *Publ. Astron. Soc. Pacific* 89, pp. 597-611.
- Bok, B.J.: 1978, *Publ. Astron. Soc. Pacific* 90, pp. 489-490.
- Bok, B.J., and Cordwell, C.S.: 1973, in M.B. Gordon and L.E. Snyder (eds.), "Molecules in the Galactic Environment," John Wiley and Sons, New York, pp. 54-90.
- Bok, B.J., Cordwell, C.S., and Cromwell, R.H.: 1971, in B.T. Lynds (ed.) "Dark Nebulae, Globules, and Protostars," University of Arizona Press, Tucson, pp. 33-55.
- Bok, B.J., and McCarthy, C.C.: 1974, *Astron. J.* 79, pp. 42-44.
- Bok, B.J., and Reilly, E.F.: 1947, *Astrophys. J.* 105, pp. 255-257.
- Bok, B.J., Sim, M.E., and Hawarden, T.G.: 1977, *Nature* 266, pp. 145-147.
- Buff, J., Gerola, H., and Stellingwerf, R.F.: 1979, *Astrophys. J.* 230, pp. 839-846.
- Carrasco, L., Strom, S.E., and Strom, K.M.: 1973, *Astrophys. J.* 182, pp. 95-109.
- Cohen, M.: 1973a, *Monthly Notices Roy. Astron. Soc.* 161, pp. 97-104.
- Cohen, M.: 1973b, *Monthly Notices Roy. Astron. Soc.* 161, pp. 105-111.
- Cohen, M.: 1975, *Monthly Notices Roy. Astron. Soc.* 173, pp. 279-293.
- Cohen, M.: 1980, *Monthly Notices Roy. Astron. Soc.* 191, pp. 499-509.
- Cohen, M., and Kuhl, L.V.: 1979, *Astrophys. J. Suppl.* 41, pp. 743-843.
- Dickman, R.L.: 1977, *Sci. Am.* 236(6), pp. 66-81.
- Dickman, R.L. 1978a, *Astron. J.* 83, pp. 363-372.
- Dickman, R.L. 1978b, *Astrophys. J. Suppl.* 37, pp. 407-427.
- Elias, J.H.: 1978a, *Astrophys. J.* 223, pp. 859-875.
- Elias, J.H.: 1978b, *Astrophys. J.* 224, pp. 453-472.
- Elias, J.H.: 1978c, *Astrophys. J.* 224, pp. 857-872.
- Elmegreen, B.G., and Lada, C.J.: 1977, *Astrophys. J.* 214, pp. 725-741.
- Feast, M.W., and Glass, I.S.: 1973, *Monthly Notices Roy. Astron. Soc.* 164, pp. 35P-38P.
- Feinstein, A., Marrace, H.G., and Muzzio, J.C.: 1973, *Astron. Astrophys. Suppl.* 12, pp. 331-350.
- Fridlund, C.V.M., Van Duinen, R.J., Nordh, H.L., Sargent, A.I., and Aalders, J.W.G.: 1980, *Astron. Astrophys.* (submitted).
- Glass, I.S.: 1979, *Monthly Notices Roy. Astron. Soc.* 187, pp. 305-310.
- Glass, I.S., and Penston, M.V.: 1975, *Monthly Notices Roy. Astron. Soc.* 172, pp. 227-233.
- Grasdalen, G., Joyce, R., Knacke, R.F., Strom, S.E., and Strom, K.M.: 1975, *Astron. J.* 80, pp. 117-124.
- Grasdalen, G.L., Strom, K.M., and Strom, S.E.: 1973, *Astrophys. J. Letters* 184, pp. L53-L57.
- Hardie, R.H., and Crawford, D.L.: 1961, *Astrophys. J.* 133, pp. 843-859.
- Harvey, P.M., Thronson, H.D., and Gatley, I.: 1979, *Astrophys. J.* 231, pp. 115-123.
- Henize, K.G.: 1963, *Astron. J.* 68, p. 280.
- Henize, K.G., and Mendoza, V.E.E.: 1973, *Astrophys. J.* 180, pp. 115-119.

- Herbig, G.H.: 1969, in L. Detre (ed.), "Non-Periodic Phenomena in Variable Stars," Academic Press, Budapest, pp. 75-82.
- Herbst, W., and Assousa, G.E.: 1977, in T. Gehrels (ed.), "Protostars and Planets," University of Arizona Press, Tucson, pp. 368-383.
- Herbst, W., and Turner, D.G.: 1976, *Publ. Astron. Soc. Pacific* 88, pp. 308-311.
- Hoffmeister, C.: 1962, *Z. Astrophys.* 55, pp. 290-300.
- Hyland, A.R., and Jones, T.J.: 1980, Paper presented at IAU Symposium 96.
- Jenkins, E.B., and Savage, B.D.: 1974, *Astrophys. J.* 187, pp. 243-255.
- Jones, T.J., and Hyland, A.R.: 1980, *Monthly Notices Roy. Astron. Soc.* (in press).
- Jones, T.J., Hyland, A.R., Robinson, G., Smith, R., and Thomas, J.A.: 1980, *Astrophys. J.* (in press).
- Joy, A.H.: 1945, *Astrophys. J.* 102, pp. 168-195.
- Jura, M.: 1979, *Astrophys. Letters* 20, pp. 89-91.
- Keene, J., Harper, D.A., Hildebrand, R.H., and Whitcomb, S.E.: 1980 (preprint).
- Kenyon, S., and Starrfield, S.: 1979, *Publ. Astron. Soc. Pacific* 91, pp. 271-275.
- Knacke, R.F., Strom, K.M., Strom, S.E., Young, E., and Kunkel, W.: 1973, *Astrophys. J.* 179, pp. 847-854.
- Lada, C.J., and Elmegreen, B.G.: 1979, *Astron. J.* 84, pp. 336-340.
- Larson, R.B.: 1972, *Monthly Notices Roy. Astron. Soc.* 157, pp. 121-145.
- Loren, R.B.: 1979, *Astrophys. J.* 227, pp. 832-852.
- Martin, R.N., and Barrett, A.H.: 1978, *Astrophys. J. Suppl.* 36, pp. 1-51.
- Mendoza, V.E.E.: 1966, *Astrophys. J.* 143, pp. 1010-1014.
- Mendoza, V.E.E.: 1968, *Astrophys. J.* 151, pp. 977-989.
- Mould, J.R., and Ridgway, S.: 1980, Private communication.
- Rydgren, A.E.: 1976, *Publ. Astron. Soc. Pacific* 88, pp. 111-115.
- Rydgren, A.E.: 1980, *Astron. J.* 85, pp. 444-450.
- Rydgren, A.E., Strom, S.E., and Strom, K.M.: 1976, *Astrophys. J. Suppl.* 30, pp. 307-336.
- Schmidt, E.G.: 1975, *Monthly Notices Roy. Astron. Soc.* 172, pp. 401-409.
- Schwartz, R.D.: 1977, *Astrophys. J. Suppl.* 35, pp. 161-170.
- Smith, R.: 1980, Private communication.
- Spencer, R.G., and Leung, C.M.: 1978, *Astrophys. J.* 222, pp. 140-152.
- Strom, K.M., Strom, S.E., Carrasco, L., and Vrba, F.J.: 1975, *Astrophys. J.* 196, pp. 489-501.
- Strom, K.M., Strom, S.E., and Vrba, F.J.: 1976, *Astron. J.* 81, pp. 308-316.
- Strom, S.E.: 1977, "Star Formation," in T. De Jong and A. Maeder (eds.), IAU Symposium 75, D. Reidel Publ. Co., Dordrecht, pp. 179-197.
- Strom, S.E., Grasdalen, G.L., and Strom, K.M.: 1974, *Astrophys. J.* 191, pp. 111-142.
- Strom, S.E., Strom, K.M., and Grasdalen, G.L.: 1975, *Ann. Rev. Astron. Astrophys.* 13, pp. 187-216.
- Strom, S.E., Vrba, F.J., and Strom, K.M.: 1976, *Astron. J.* 81, pp. 314-316.
- Tapia, S.: 1975, in Greenberg and Van de Hulst (eds.), IAU Symposium 52, "Interstellar Dust and Related Topics," D. Reidel Publ. Co., Dordrecht, pp. 43-51.

- Tomita, Y., Saito, T., and Ohtani, H.: 1979, Publ. Astron. Soc. Japan 31, pp. 407-416.
- Villere, K.R., and Black, D.C.: 1980, Astrophys. J. 236, pp. 192-200.
- Vrba, F.J.: 1976, Ph.D. Thesis, University of Arizona, Tucson.
- Vrba, F.J.: 1977, Astron. J. 82, pp. 198-208.
- Vrba, F.J., Strom, K.M., Strom, S.E., and Grasdalen, G.L.: 1975, Astrophys. J. 197, pp. 77-84.
- Vrba, F.J., Strom, S.E., and Strom, K.M.: 1976, Astron. J. 81, pp. 317-319.
- Walraven, Th., and Walraven, J.H.: 1960, Bull. Astron. Inst. Neth. 15, pp. 67-83.
- Werner, M.W., and Salpeter, E.E.: 1969, Monthly Notices Roy. Astron. Soc. 145, pp. 249-269.
- Wootten, A., Evans, N.J., II, Snell, R., and Vanden Bout, P.: 1978, Astrophys. J. Letters 225, pp. L143-L148.

## DISCUSSION FOLLOWING PAPER PRESENTED BY A. R. HYLAND

NORDH: The dust temperature, 13-16 K, quoted for B335 is higher than previously quoted by Keene et al., and also higher than existing theoretical predictions of dust temperatures of dark clouds illuminated by the ISM (see Leung, Ap.J. 199, 340, 1975). Do you or Keene have any comments to this?

KEENE: There are new observations which give a slightly higher temperature than 10 K. I don't believe there is a significant difference between the temperature we observe and the theoretical models.

LADA: The far-IR observations of Keene et al. are in very good agreement with theoretical predictions. For example, a few years ago Leung calculated dust temperature distributions for clouds heated by the general background radiation field. He found that the dust temperatures range from ~12 K to 2 K from the surface to core of the clouds. Therefore the observed temperature  $T_D = 13-16$  K for B335 is entirely compatible with expectations. Also for these objects the gas and dust temperatures are not necessarily coupled. Gas is heated by cosmic rays and cooled by line emission with equilibrium gas temperatures of ~8-12 K. Dust is heated by starlight and cooled by thermal re-radiation to temperatures between 7 and 14 K. The fact that the two are roughly equal is mostly fortuitous and not an indication of a common physical basis for heating.

SHERWOOD: We have detected B68 at 1 mm (300-330 GHz). The observations are in agreement with thermal emission from dust at 10 K.